Numerical Simulation of Wave Propagation Using the Shallow Water Equations

Junbo Park

Harvey Mudd College

26th April 2007

Abstract

The shallow water equations (SWE) were used to model water wave propagation in one dimension and two dimensions. SWE were approximated by using finite difference method. One dimensional SWE were tested using various initial conditions. 1D and 2D SWE were used to model tsunami wave propagation near coast line. 1D model correctly predicts the behavior of tsunami water wave. 2D model develops numerical oscillation once the wave reaches shallow area. A real basin data from Gulf of Mexico has been tested to simulate the wave propagating in the area.

The shallow water equations describe propagation of water wave whose wavelength is much longer than the depth of water. Tsunamis are examples of such waves. Wavelength of a typical tsunami can exceed 100 km. This is to be compared with the average depth of ocean which is approximately 5 km [1]. Therefore, tsunami wave propagation can be modeled using shallow water equations. In this report, we use a numerical method to simulate wave propagation in one and two dimensions. The same scheme is used to model tsunami wave propagation near a shore.

Shallow Water Equations

The derivation of the shallow water equations follows from the conservation of mass and momentum. In deriving the equations, however, we must make an assumption about the water that is being modeled. We assume that there is no pressure variation in the vertical direction[2]. Therefore, it cannot correctly model the behavior of a water fall. This naturally forces the wavelength of the water wave to be larger than the depth of the water. Furthermore, in this report, we neglected friction between the fluid and the basin. However, friction can actually be accounted for—Imamura et al. have successfully modeled the frictional contribution[3].

One dimensional Shallow Water Equations

The shallow water equations in one dimension are

$$\frac{\partial \eta}{\partial t} + \frac{\partial M}{\partial x} = 0 \tag{1.a}$$

$$\frac{\partial M}{\partial t} + \mathrm{g}D\frac{\partial \eta}{\partial x} = 0. \tag{1.b}$$

where g is the gravitational constant, D is the total thickness of water at x, and M is a quantity defined as product of depth averaged velocity and water velocity in the $+x$ direction[4]. Equation (1.a) and (1.b) are manifestation of mass and momentum conservation law, respectively. As mentioned earlier, frictional terms have been ignored in our discussion of SWE.

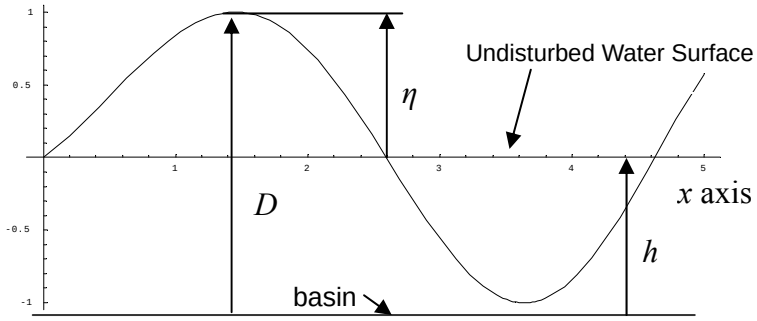

Fig 1. Water level profile of an example 1D wave

The shallow water equations are coupled first order differential equations that can be uncoupled to produce two second-order differential equations.

$$\frac{\partial^2 M}{\partial t^2} = g(\eta + h)\frac{\partial^2 M}{\partial x^2} - \frac{1}{\eta + h}\frac{\partial^2 M}{\partial t \partial x} \tag{2.a}$$

$$\frac{\partial^2 \eta}{\partial t^2} = g(\eta + h)\frac{\partial^2 \eta}{\partial x^2} + g\left(\frac{\partial \eta}{\partial x}\right)^2 + \frac{\partial h}{\partial x}\frac{\partial \eta}{\partial x} \tag{2.b}$$

where h is the depth of the water—the relation between D and h is $D = h + \eta$. The form of equation (2.a) and (2.b) is very similar to that of a wave equation. The speed of η and M propagation at given x is, therefore, determined by total thickness of water, $D(x)$—$c_s^2 \approx gD = g(\eta + h)$.

Numerical Scheme for 1D Shallow Water Equations

To solve the shallow water equations numerically, we first discretized space and time. We used finite differences to approximate the spatial and time derivatives. The time derivatives were approximated by using the second-order centered differences following the Crank-Nicolson method. The spatial derivatives were approximated by using the second-order centered differences. For the one dimensional SWE, we used a semi-implicit and implicit method to compare the numerical stability of solution. For all 1D simulations, we used spatial grid size Δx = 1/8 m and time step size Δt = 1/3000 sec.

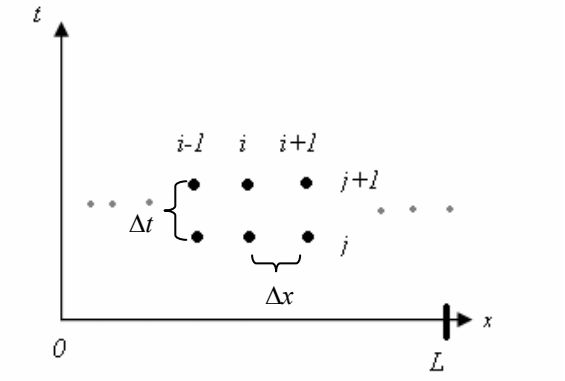

Fig 2. Spatial and time discretization. Spatial domain is discretized using $Nx + 1$ points ($Nx = L/\Delta x$).

The boundary condition imposed on $x = 0$ and $x = L$ are given as

$$M = 0$$
$$\eta_0^j = \eta_1^j;\ \eta_{Nx-1}^j = \eta_{Nx}^j . \tag{3}$$

where η_i^j is an approximation to $\eta(i\Delta x, j\Delta t)$. Equation (3) sets x-velocity of water to be zero at boundary. As a consequence, $\partial\eta/\partial x = 0$ at the boundary.

Semi-Implicit Method

Using finite difference method, we can approximate equation (1) as

$$M_i^{j+1} = M_i^j - (1/2)\mathrm{cg}(\eta_i^j + h_i)(\eta_{i+1}^j - \eta_{i-1}^j) \tag{4.a}$$
$$\eta_i^{j+1} = \eta_i^j - (\mathrm{c}/4)(M_{i+1}^{j+1} - M_{i-1}^{j+1}) - (\mathrm{c}/4)(M*_{i+1}^{j+1} - M*_{i-1}^{j+1}) \tag{4.b}$$

where $\mathrm{c} = \Delta t/\Delta x$, the ratio between time step and spatial step. M_i^j is an approximation to $M(i\Delta x, j\Delta t)$. Given an initial condition at time $t = 0$, this method can be used to compute η and M at subsequent time steps.

However, this numerical scheme is not an explicit method, but rather a semi-implicit method. To compute M_i^{j+1}, we use η's from previous time step j. To compute η_i^{j+1}, however, we use $M*_{i+1}^{j+1}$ and $M*_{i-1}^{j+1}$ which is obtained by solving equation (4.a) for M_i^{j+1} first.

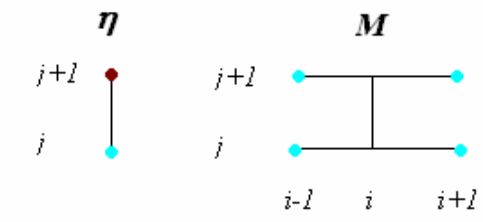

Fig 3. Stencil of Semi-Implicit method for computing η.

Implicit Method

To increase the numerical stability of the solution, we have implemented an implicit method on the one dimensional shallow water equations. However, equation (1.b) is non-linear since $D = \eta + h$. In order to implement an implicit scheme, (1.b) had to be separated into linear part and non-linear part. Applying Crank-Nicolson method and finite difference method, we obtain following equation:

$$\begin{aligned} M_i^{j+1} + (1/4)\mathrm{cg}h_i(\eta_{i+1}^{j+1} - \eta_{i-1}^{j+1}) &= M_i^j - (1/2)\mathrm{cg}\eta_i^j(\eta_{i+1}^j - \eta_{i-1}^j) - (1/4)\mathrm{cg}h_i(\eta_{i+1}^j - \eta_{i-1}^j) \\ \eta_i^{j+1} + (\mathrm{c}/4)(M_{i+1}^{j+1} - M_{i-1}^{j+1}) &= \eta_i^j - (\mathrm{c}/4)(M_{i+1}^{j+1} - M_{i-1}^{j+1}) \end{aligned} \qquad (5)$$

Left hand sides of equation 5 are M and η terms at time step $j+1$. The right hand sides are terms at time step j. Values of M and η at time step $j+1$ can be computed by solving a linear system of equations.

Test of 1D Shallow Water Equations

The shallow water equations in one dimension were tested with three different initial conditions. In all cases, the initial velocity of the water was set to be zero—water was at rest at $t = 0$, and therefore $M = 0$. We varied $\eta(t = 0)$ to examine the results of numerical simulations. The first row in Figure 4 illustrates the three different $\eta(\mathrm{t} = 0)$'s. The solutions at later time t are plotted in the second row. The solutions obtained by using semi-implicit method and explicit method are plotted on the same graph for each plot. Note that the solutions almost overlap each other.

We observe that the solution to initial condition in Figure 4(a) and 4(b) develop numerical instabilities. However, these numerical instabilities are not inherent to shallow water equation. Equation (1) is a differential form of shallow water equation which assumes that the water profile is smooth. Yet, the initial conditions given are not necessarily smooth. This can be understood if we examine equation (2).

From equation (2) which resembles a wave equation, we can deduce that the solution to shallow water equation can be approximated with superposition of sinusoids. Therefore, the initial profile of η can be thought of as a superposition of sinusoids. The step function, however, can be expressed with very high frequency sinusoids. Those high frequency components develop into numerical oscillations. Yet the original shallow water equation allows for discontinuous solutions such as a bore[5]. To solve problems with non-smooth profile, finite volume method should be used.

The numerical oscillation we observe does not arise from instability of semi-implicit method, either. Implicit method does not improve the results. The solutions are nearly exactly the same. The numerical instability arises from the limits of finite difference method.

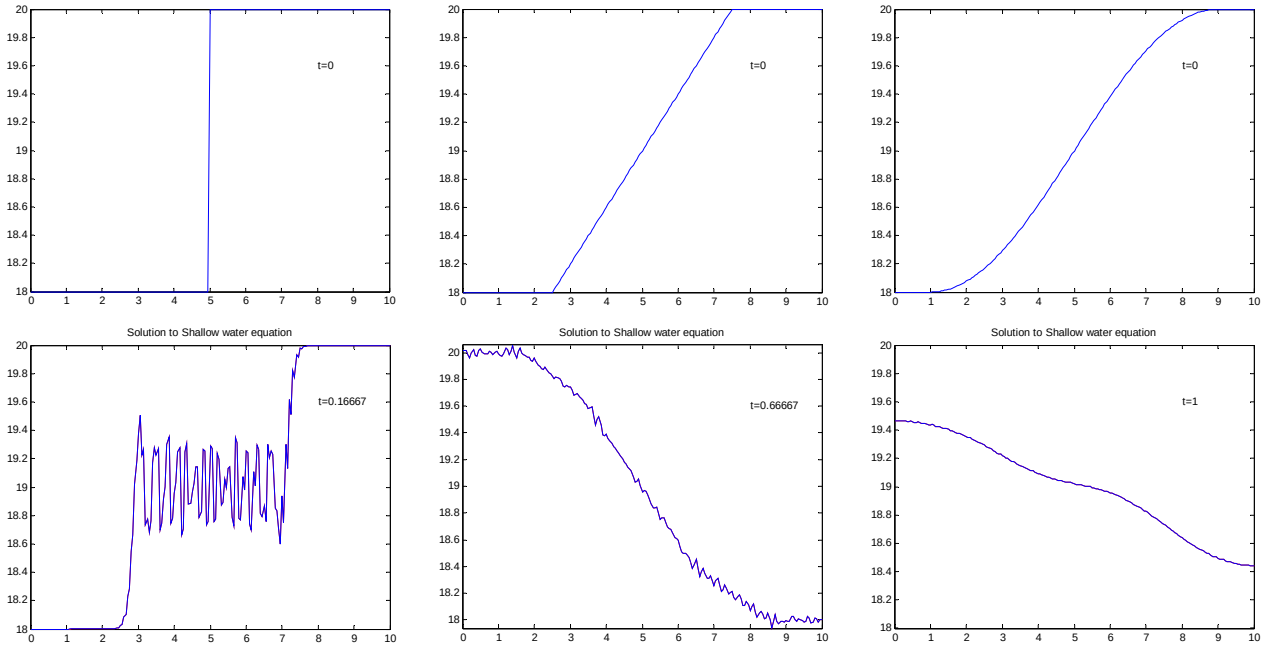

(a) (b) (c)

Fig 4. Three different initial η conditions: step function, slope, sinusoid are plotted in the first row. The second row is plots of η at later time step. Results from using explicit method and implicit method have been plotted. The maximum and minimum value of $\eta(t=0)$ are 18m and 20m respectively. The basin depth is 0m for all three cases. (a) $\eta(t=0)$ and $\eta(t=0.167)$. (b) $\eta(t=0)$ and $\eta(t=0.667)$. (c) $\eta(t=0)$ and $\eta(t=1)$.

Finite difference method assumes that derivatives exist at all points. Therefore, it cannot handle discontinuous initial condition such as step function. It also cannot produce stable solutions for initial conditions described in figure 4(b) since the derivative of the initial condition is discontinuous. As observed in figure 4(a) and 4(b), numerical instability ensues if the initial condition profile is not twice differentiable. When given a sinusoid as an initial condition, the solution remains stable for much longer period.

Tsunami wave in 1D

The shallow water equations were used to model wave propagation near the shore. The basin profile has been approximated by a hyperbolic tangent given as

$$h(x) = 50 - 45\tanh\left(\frac{x-70}{8}\right) \qquad 0\text{ m} \le x \le 100\text{ m} \quad (6)$$

such that the depth would range from 5m to 95m. We made the depth of water to be positive at all

x since very high numerical error occurs if we let depth profile be negative—this would correspond to above sea level. The initial condition was given as a Gaussian for η and M

$$\eta(x,0) = 0.5\exp(-(x-20)^2/8);$$
$$M(x,0) = 50\exp(-(x-20)^2/8) = 100\,\eta(x,0); \tag{7}$$

M was given a non-zero value to make the wave propagate to $+x$ direction.

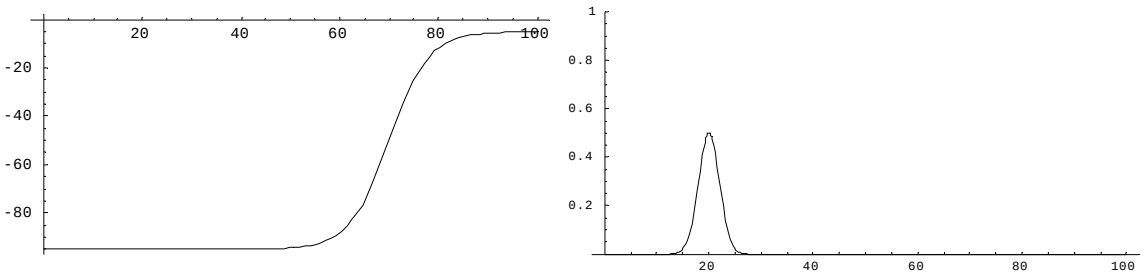

(a) (b)

Fig 5. (a) Plot of $-h$, the depth profile used in the simulation. (b) Initial condition for η and 0.01 M.

The result of this simulation is plotted in Figure 6. As the wave approaches the shore and enters the shallower area, the wave slows down. This is what was expected since the wave propagation speed is approximately $c_s^2 = gD$ (see equation (2)). As the wave slows down, the width of the Gaussian wave packet is reduced. This results in increased amplitude of the water wave.

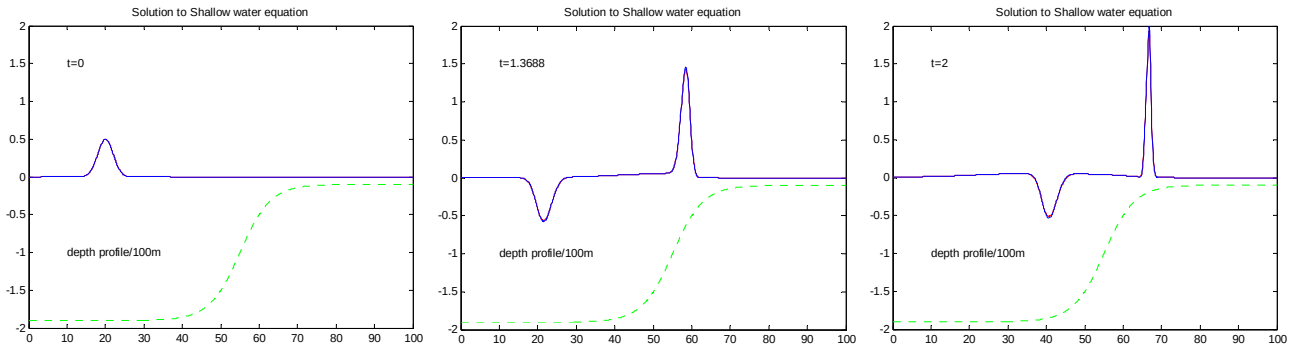

(a) (b) (c)

Fig 6. η at various time step. The depth profile has been scaled down by a factor of 100 (a) $t = 0$. (b) $t = 1.37$ (a) $t = 2$

Two Dimensional SWE

Shallow water equations in 2D are extensions to 1D equations. The set of equations are given as

$$\frac{\partial \eta}{\partial t}+\frac{\partial M}{\partial x}+\frac{\partial N}{\partial y}=0 \tag{8.a}$$

$$\frac{\partial M}{\partial t}+\frac{\partial}{\partial x}\left(\frac{M^2}{D}+\frac{1}{2}\mathrm{g}\eta^2\right)+\frac{\partial}{\partial y}\left(\frac{MN}{D}\right)+\mathrm{g}h\frac{\partial \eta}{\partial x}=0 \tag{8.b}$$

$$\frac{\partial N}{\partial t}+\frac{\partial}{\partial x}\left(\frac{MN}{D}\right)+\frac{\partial}{\partial y}\left(\frac{N^2}{D}+\frac{1}{2}\mathrm{g}\eta^2\right)+\mathrm{g}h\frac{\partial \eta}{\partial y}=0 \tag{8.c}$$

where N is product of D and depth averaged velocity in $+y$ direction[6]. Equation (8.a) is derived from mass conservation law. Equation (8.b) and (8.c) are derived from momentum conservation law. Friction has been ignored in these equations.

Numerical Scheme for Two Dimensional SWE

The numerical method used for two dimensional SWE was very similar to that of one dimensional case. Space and time have been discretized into a grid. The size of the spatial domain was determined to be a 100m by 100m. The spacing between each grid point, Δx and Δy, was set to be 1m. The size of the time step was set to be Δt = 1/4000 sec.

We used finite difference method to approximate 2D SWE. The spatial derivatives were approximated by using the second-order centered differences. The time derivatives were approximated by using the second-order centered differences following the Crank-Nicolson method.

Equation (8), therefore, can be approximated by

$$\begin{aligned}&\eta_{i,j}^{k+1}+(1/4)\mathrm{c}_x(M_{i+1,j}^{k+1}-M_{i-1,j}^{k+1})^{*}+(1/4)\mathrm{c}_y(N_{i,j+1}^{k+1}-N_{i,j-1}^{k+1})^{*}\\&=\eta_{i,j}^{k}-(1/4)\mathrm{c}_x(M_{i+1,j}^{k}-M_{i-1,j}^{k})-(1/4)\mathrm{c}_y(N_{i,j+1}^{k}-N_{i,j-1}^{k})\end{aligned} \tag{9.a}$$

$$M_{i,j}^{k+1}=M_{i,j}^{k}-(1/2)\mathrm{c}_x\left(\left(\frac{M^2}{D}\right)_{i+1,j}^{k}-\left(\frac{M^2}{D}\right)_{i-1,j}^{k}+(\mathrm{g}/2)((\eta_{i+1,j}^{k})^2-(\eta_{i-1,j}^{k})^2)\right)-(1/2)\mathrm{c}_y\left(\left(\frac{MN}{D}\right)_{i,j+1}^{k}-\left(\frac{MN}{D}\right)_{i,j-1}^{k}\right)$$
$$-\mathrm{g}h_{i,j}(1/2)\mathrm{c}_x(\eta_{i+1,j}^{k}-\eta_{i-1,j}^{k}) \tag{9.b}$$

$$N_{i,j}^{k+1}=N_{i,j}^{k}-(1/2)\mathrm{c}_y\left(\left(\frac{N^2}{D}\right)_{i,j+1}^{k}-\left(\frac{N^2}{D}\right)_{i,j-1}^{k}+(\mathrm{g}/2)((\eta_{i,j+1}^{k})^2-(\eta_{i,j-1}^{k})^2)\right)-(1/2)\mathrm{c}_x\left(\left(\frac{MN}{D}\right)_{i+1,j}^{k}-\left(\frac{MN}{D}\right)_{i-1,j}^{k}\right)$$
$$-\mathrm{g}h_{i,j}(1/2)\mathrm{c}_y(\eta_{i,j+1}^{k}-\eta_{i,j-1}^{k}) \tag{9.c}$$

Again, the * in equation (9.a) indicates that the values of M and N at time step $j+1$ are from calculating M and N first using equation (9.b) and (9.c).

The boundary conditions are similar to that of 1D case. M and N are zero on the

x-y boundaries—this is also known as no slip condition. Water cannot move into or out of a boundary. It also cannot move along a boundary.

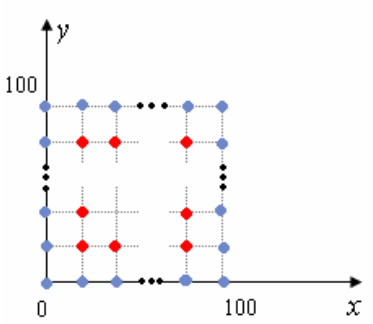

Fig 7. Layout of discretized grid. The value of η at the boundary points (blue dot) are always equated to the value of η inside the boundary (red dot) at each time step.

Simple Model: Hyperbolic Tangent Basin

The 2D shallow water equations were used to simulated water wave near a shore. The sea basin was modeled as a hyperbolic tangent. The depth profile was given as

$$h(x,y) = 50 - 45\tanh\left(\frac{-(x-50)^2}{20}\right). \tag{10}$$

The initial condition was given as

$$\eta(x,y,0) = 0.5\exp(-\frac{(x-30)^2}{10} - \frac{(y-50)^2}{20})$$
$$M(x,y,0) = 100\,\eta(x,y,0) \tag{11}$$

The result of numerical simulation is shown in figure 8. The initial Gaussian profile pans out into the *x-y* plane in all direction. Bulk of the water, however, travels toward +*x* direction. There are features that are common to the 1D and 2D results. The waves slows down

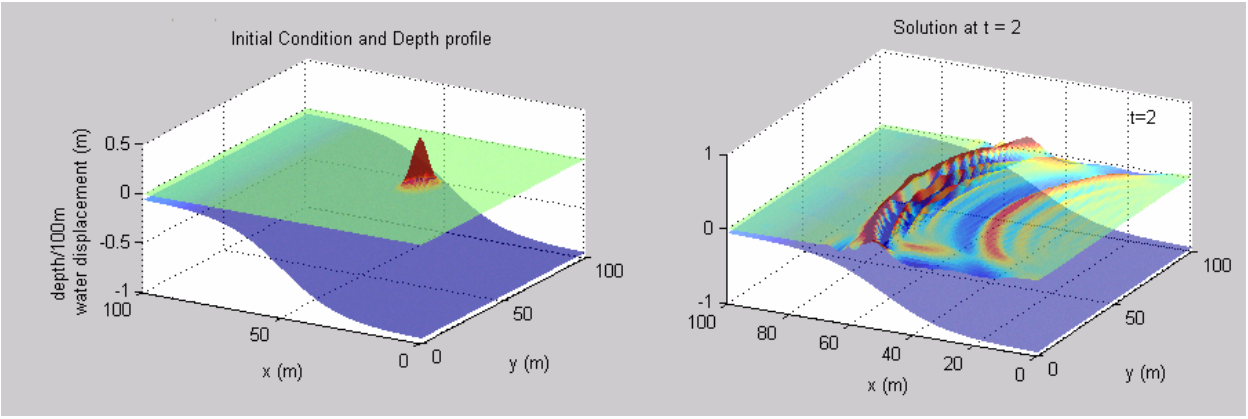

(a) (b)

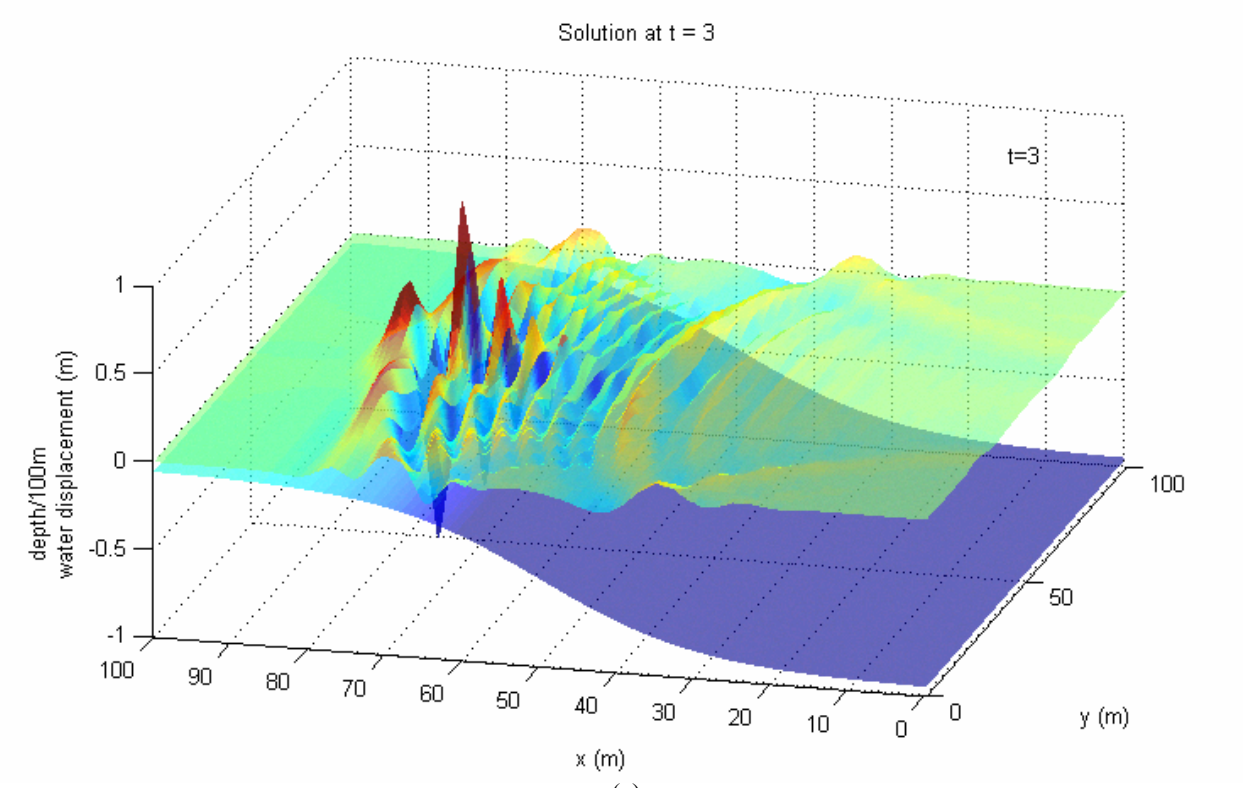

(c)

Fig 8. Numerical simulation of water propagation near coast line. (a) Solution at $t = 0$. (b) Solution at $t = 2$ sec. (c) Solution at $t = 3$ sec

as it approaches the shore. Note that the wave front barely moved between $t = 2$ and $t = 3$. Also, the amplitude of the water increase as the wave packet approaches the shore.

Unlike the 1D case, however, we see more severe numerical oscillation occurring as the wave approaches the shore. Numerical oscillation is visible in solution at $t = 2$, and it becomes more pronounced as the wave front approaches shallower parts of the shore at $t = 3$. Implicit method has not been implemented to check if this was an artifact of semi-implicit scheme that we used to solve two dimensional SWE. However, we know from the results of 1D SWE simulations that using implicit method does not guarantee a stable solution.

One possible source of numerical oscillation may be the discrepancy between analytical domain of dependence and numerical domain of dependence. In a hyperbolic equation, information travels at the speed of wave propagation. Figure 9 illustrates the domain of dependence of two kind: analytic and numerical. Numerical domain of dependence is determined by the grid spacing Δx and the method used to approximate the derivatives. Analytic domain of dependence is determined by the speed of the wave propagation, c_s, and the time step size. When two domain of dependence differ from another greatly, numerical error is induced. In hyperbolic equations, this leads to dispersive behavior of the numerical solution[7]. Waves with different wavelength travel at different speed.

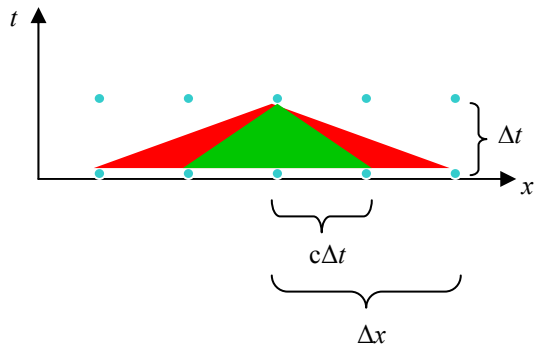

Fig 9. Schematic diagram of analytic domain of dependence and numerical domain of dependence. In this case, analytical domain of dependence is narrower than the numerical domain of dependence.

However, as equation (2) suggests, shallow water equations have the form of a hyperbolic equation. Furthermore, c_s is determined by the depth of the water: $c_s^2 = gD$. Therefore, as the waves approach the shallower region, the analytical domain of dependence becomes narrower than numerical domain of dependence. This results in dispersive behavior which makes waves with different wave length travel at different speed. Since a Gaussian wave packet is a superposition of many sinusoids, the wave breaks down into discrete waves traveling at different speed. The result is numerical oscillation which is a manifestation of interference between various sinusoidal waves.

Gulf of Mexico

The two dimensional shallow water equations were further tested, using a real basin data which can be obtained from National Geophysical Data Center website[8]. We obtained the depth profile of sea basin near the Gulf of Mexico. The bathymetric profile was sampled at discrete points separated by approximately 4000m. The size of the basin area was 400 km by 400 km. The depth ranged from 50m to 2 km.

The raw bathymetry data, however, could not be used because the profile was not "smooth" enough. The jagged terrains, which is a product of coarse resolution of grid cell (Δx, Δy = 4 km), was a major source of numerical instability. In order to smooth out the terrain, and yet retain the original profile, we applied convolution to each data point.

$$h_{i,j}^{*} = \sum_{k,l}^{N+1} S_{i,j}(k\Delta x, l\Delta y) \cdot h_{k,l} \tag{12}$$

where $h_{i,j}$* is the smoothed depth profile at $x = i\Delta x$ and $y = j\Delta y$. $S_{i,j}$(x, y) is given as

$$S_{i,j}(x,y) = \frac{1}{2\pi}\exp\left(-\frac{(x-i\Delta x)^2 + (y-j\Delta y)^2}{4}\right). \tag{13}$$

Equation 12 is a discrete form of convolution. The result of this is shown in Figure 10.

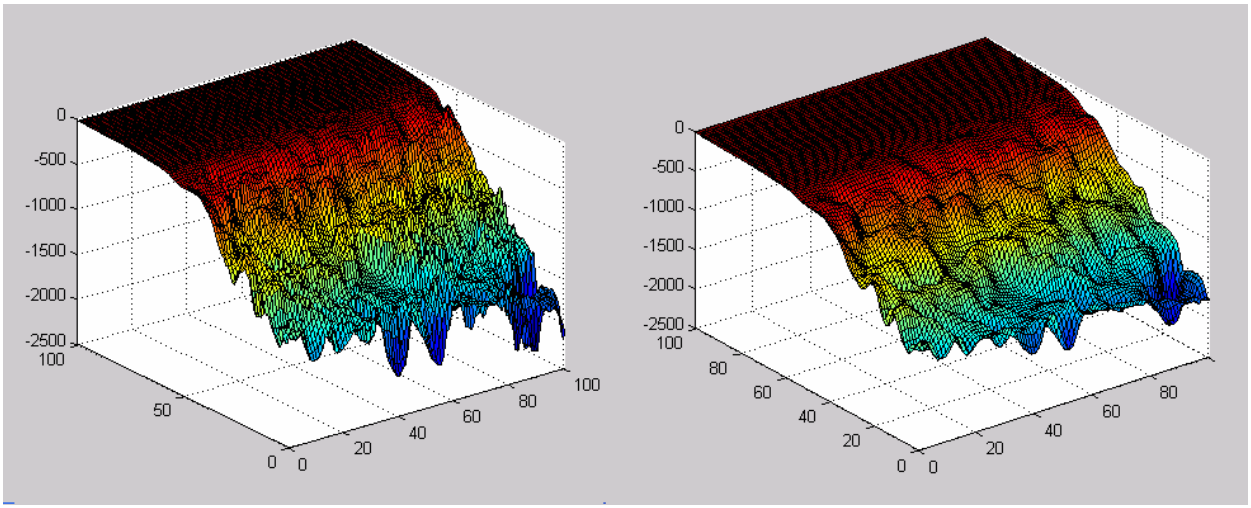

(a) (b)

Fig 10. (a) Raw depth profile. (b) Product obtained after applying convolution

The initial condition for this simulation was given as

$$\eta(x,y,0) = 0.5\exp\left[-\left(\frac{x-80000}{20000}\right)^2 - \left(\frac{y-200000}{40000}\right)^2\right]$$
$$M(x,y,0) = 50\,\eta(x,y,0) \qquad (14)$$

The results of numerical simulation are plotted in Figure 11.

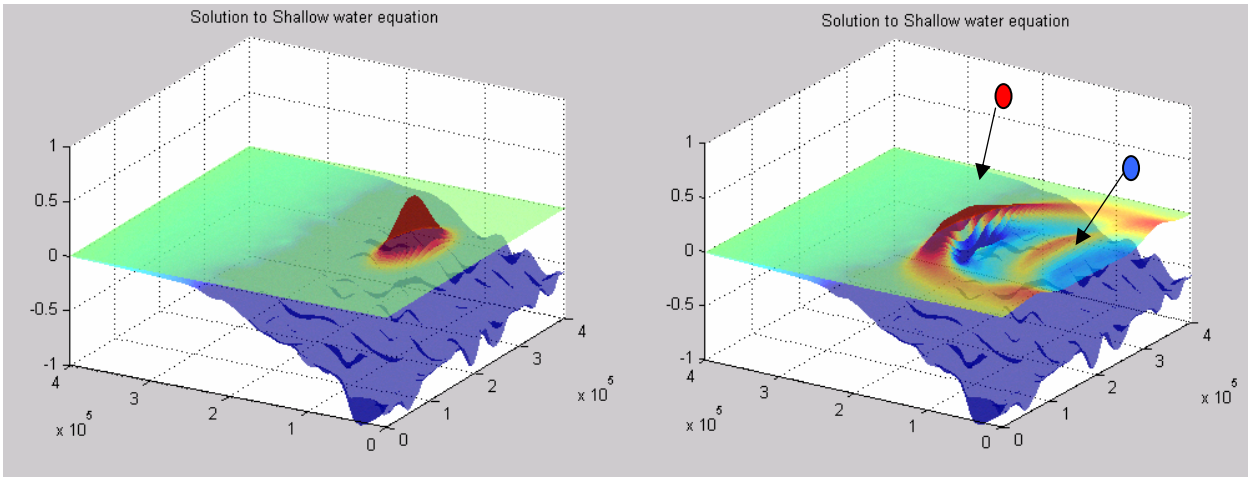

(a) (b)

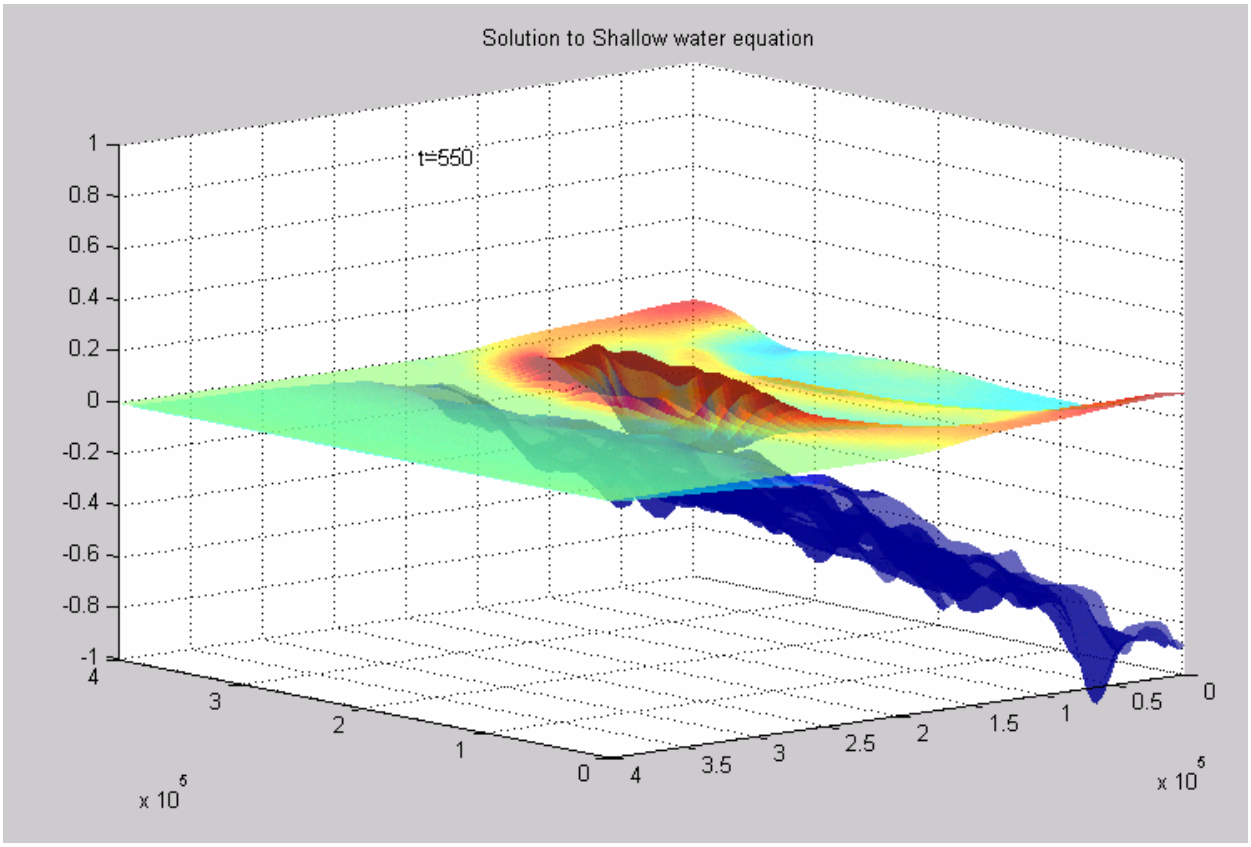

(c)

Fig 11. Wave propagation in Gulf of Mexico (a) Initial condition and sea basin (b) Solution at $t = 400$ sec. (c) Solution at $t = 550$ sec. The lateral ripples are not due to numerical oscillation. The ripples arise from the shape of the basin. Compare this with figure 8(c).

The lateral ripples observed in Figure 11(c) are due to the shape of basin. This type of ripples does not develop when the depth profile is a simple hyperbolic tangent given in equation (10). Such ripples are not observed in Figure 8(c). The curves observed in Figure 8(c) is due to waves that reflected from the $y = 0$ and $y = 100$m boundary.

The solution, however, quickly becomes unstable as soon as the waves reflected from $x = 0$ catches up with the original wave—in Figure 11(b), the original wave is labeled with red circle and the reflected wave is labeled with blue circle. Interference between two waves produces numerical oscillations.

Acknowledgement

I would like to thank Professor Yong for providing me with resources and guiding me through out the project. I thank Sean Meenehan for guiding me to find resources about bathymetry data. I thank Nick Alger for his idea of applying convolution to raw bathymetric data.

References

[1] http://www.geophys.washington.edu/tsunami/general/physics/characteristics.html

[2] Kevorkian, J. *Partial Differential Equations: Analytic Solution Techniques*. Pacific Grove, Calif., c1990. pp 120-9.

[3] Imamura, F., Yalciner, A.C., *Tsunami Modeling Manual (Draft)*. 2006. pp. 7-8.

[4] Imamura,F. et al. pp 9

[5] Kervorkian, pp. 122-3.

[6] Imamura,F. et al. pp 6-7

[7] Yong, D. *Private Communication (Scientific Computing Lecture 2007)*.

[8] http://www.ngdc.noaa.gov/mgg/bathymetry/relief.html